Sensitivity of physical parameterization schemes in WRF model for dynamic downscaling of climatic variables over the MRB

Lia Pervin and Thian Yew Gan

ABSTRACT

The Weather Research and Forecasting (WRF) model was tested through 18 different combinations of physics parameters to simulate the regional climate over the Mackenzie River Basin (MRB). The objective was to investigate the response to the physics parameters for dynamic downscaling of climatic variables. The rainfall, temperature, albedo, and surface pressure from the 18 different WRF setups were compared with the reference data and were found sensitive to land surface physics and microphysics and to the radiation physics. The combination of Noah Land Surface Physics with the WRF Single-moment 6-class microphysics and CAM shortwave and longwave schemes produced comparable results for summer 2009. This WRF setup was further tested for summers 1979–1991 and it was found that WRF could simulate air temperature more accurately than the rainfall, since the rainfall over the mountainous regions was over-simulated. Then the selected combinations of WRF parameterizations were used to downscale the CanESM2 historical temperature and rainfall for summers 1979–2005, which showed good agreement with the reference data. The suggested WRF parameters from this study could be utilized for regional climate modeling of MRB.

Key words | dynamic downscaling, physical parameters, regional climate sensitivity, WRF model

Lia Pervin (corresponding author)
Department of Civil and Environmental Engineering,
University of Alberta,
Edmonton, AB,
Canada
T6G 1H9
E-mail: *liapervin@gmail.com*

Thian Yew Gan
Department of Civil and Environmental Engineering,
7-230 Donadeo Innovation Centre For Engineering,
University of Alberta,
Edmonton, AB,
Canada
T6G 1H9

HIGHLIGHTS

- This study enhances the overall understanding of the hydrology and climatic pattern of a large river basin like the MRB (1.8 million square km).
- The sensitivity test with various physics parameters gives an idea of the model behavior under different physics combinations.
- Using the fine-tuned WRF setup short-term and long-term climate data (temperature, rainfall, albedo and surface pressure) were simulated.
- The combinations of WRF parameterizations from this study could be used for comprehensive climate modeling of this region.

INTRODUCTION

Regional climate is generally well understood and can be simulated well by a mesoscale model. Selection of model parameters and the performance of a mesoscale model are subject to variation depending on the local climate and on the complexities of the terrain. It is expected that simulating any local climate of a mountainous terrain will have interactions between the overlying atmosphere and the terrain, which could affect the model performance as well. The

doi: 10.2166/wcc.2020.036

Weather Research and Forecasting (WRF) model is a next-generation mesoscale numerical weather prediction system which is being used by many researchers in different parts of the world. Several studies have been reported on the application of the WRF model. Chawla *et al.* (2018) used the WRF to simulate extreme rainfall events in the upper Ganga Basin, India and Yang *et al.* (2019) tested three different microphysics parameterizations to simulate raindrop size distribution in Chilbolton, UK. Pérez *et al.* (2014) investigated the ability of the WRF model to simulate the climate over a complex region, the Canary Islands. They found that the simulated maximum and minimum temperatures together with the daily rainfall, were comparable with the reanalysis data (ERA-Interim). They also stated that both the microphysics and the boundary layer schemes have a large impact on the simulated precipitation. Zhang *et al.* (2012) found that the WRF model can realistically simulate the magnitude and geographical distribution of the mean rainfall over the Hawaiian Islands; in addition, their model simulations reproduced the individual heavy rainfall events well. They concluded that WRF can be a useful tool for dynamical downscaling of regional climate over the Hawaiian Islands. Mooney *et al.* (2013) applied the WRF model to downscale the ERA-Interim data for the climate over Europe for the period of 1990–1995; they suggested that parameterization combinations should be carefully selected for simulating realistic climate variables such as surface air temperatures (T2), precipitation, and mean sea level pressure (MSLP). Gula & Peltier (2012) applied the WRF model to the Great Lakes system of North America and demonstrated that the more comprehensive physics options of the WRF model provided significantly improved results compared to those obtained from the global model. The model showed greater success in capturing the details of the annual cycle and spatial pattern of precipitation, as well as producing much more realistic lake-induced precipitation and snowfall patterns.

In this study, our objective was to find out how the choice of physics parameters could possibly affect the WRF model simulations over a large and complex river basin like the MRB and also how realistically WRF can simulate the long-term summer temperature and rainfall over the MRB. This effort using different WRF parameterizations for sensitivity analysis will enhance the knowledge of regional climate modeling performance.

METHODS

Study area

Mackenzie River Basin (MRB), a high latitude continental basin with a total area of about 1.8 million square kilometers, extending from 52° to 69° N and 140° W to 102° W, which enjoys being the largest river basin in Canada. The basin possesses a unique hydrological and environmental variability as it has continuous permafrost at the north and warm summer at the south. It can be described with three major physiographic regions: the Cordillera, the Interior Planes, and the Precambrian Canadian Shield. Atmospheric circulation is greatly influenced by the topography: the Rockies at the western side and the lower latitude at the central part induce strong atmospheric circulations; the lakes and wetlands affect the energy and water balance of the basin (Woo *et al.* 2008). Figure 1 shows the model domain and terrain height of the study area.

Selection of physics parameters for WRF model configuration

The WRF model is being used as a regional climate model (RCM) for dynamical downscaling of global model data in different parts of the world, because WRF provides the freedom to select the options that best describe the regional climate of interest and produces finer resolution data (even for 3 km by 3 km resolution) for that geographic region (Prabha *et al.* 2011).

The Advanced Research WRF (ARW-WRF) modeling system gives a large selection of physical parameters which makes the model more specified according to our needs. The selection of physics parameters are also influenced by the geographic position and topography of the area. Microphysics, longwave and shortwave radiation, surface layer, land surface, planetary boundary layer and also cumulus parameterization play important roles for simulating the regional climate (Mooney *et al.* 2013; Pei *et al.* 2014; Pérez *et al.* 2014).

Tests setup

The WRF model was set up to test the sensitivity of the physics parameters to simulate the climate over the MRB.

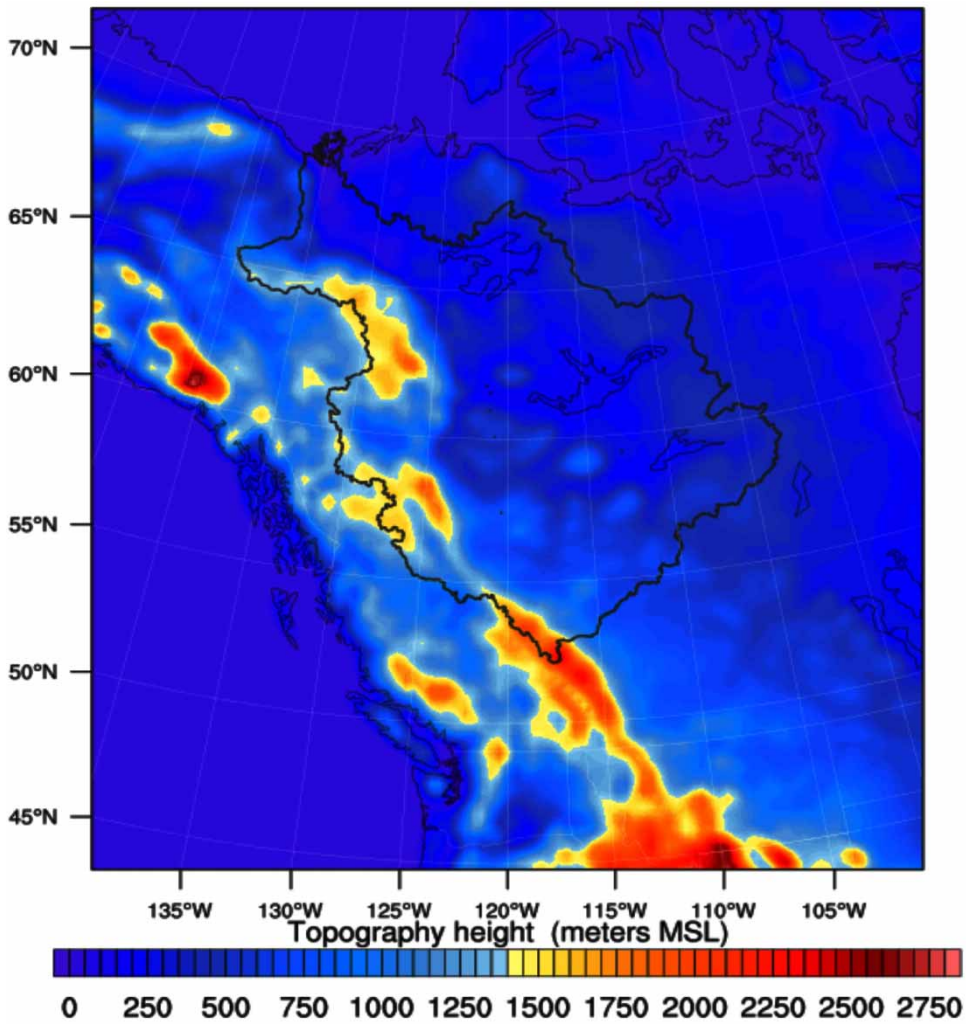

Figure 1 | Domain area with terrain height of the study area (Mackenzie River Basin is outlined on the map).

WRF domain was selected in such a way that the MRB gets the required freedom to develop its own synoptic and meso-scale circulation during the summer period. The selected domain size was 100 grids in the east–west direction and 112 grids in the north–south direction, where each grid cell is 30 km by 30 km in horizontal resolution. For the model setup and data preprocessing the USGS 24-category land data were used. A Lambert conformal projection system was selected. For the initial and boundary condition to run the WRF model, the ERA-Interim 1 degree by 1 degree data with 6 hourly time steps were used. The model was set up with 28 eta levels, which are as follows: 1.000, 0.990, 0.978, 0.964, 0.946, 0.922, 0.894, 0.860, 0.817, 0.766, 0.707, 0.644, 0.576, 0.507, 0.444, 0.380, 0.324, 0.273, 0.228, 0.188, 0.152, 0.121, 0.093, 0.069, 0.048, 0.029, 0.014, 0.000.

To set up the physics parameters three categories of land surface models were selected, which combine with other physics parameters. The Appendix shows all the physics options used in these experiments using the numerical numbering and the name. The first group is taken as the sf_surface_physics option 1, which is the 5-layer Thermal Diffusion scheme for the land surface physics. The other physics parameters were selected as the WRF Single-moment 3-class scheme, WRF Single-moment 5-class scheme, Lin *et al.* scheme for the microphysics (mp_physics) option, while RRTM scheme and RRTMG scheme were

used for longwave radiation (ra_lw_physics), and Dudhia scheme and RRTMG shortwave schemes for shortwave radiation (ra_sw_physics). These selections also combine with Yonsei University scheme and Asymmetric Convection Model 2 scheme (ACM2) for its planetary boundary layer (bl_pbl_physics) and for surface layer option MM5 Similarity scheme was chosen, and Kain–Fritsch scheme was taken as the cumulus parameterization option (cu_physics). Table 1 shows the combination of the physics parameters with 5-layer Thermal Diffusion scheme; here numerical numbers correspond to the physics scheme as mentioned in the WRF-ARW user manual.

For the second category, the Unified Noah Land Surface model was chosen as the land surface scheme, where a total of 12 different combinations of physics parameters were used. Table 2 shows the combinations of the physics parameters with Unified Noah Land Surface physics (using the same numerical numbers used in WRF).

The third category is the combinations of physics options with the RUC Land Surface Model. A total of three sets were tested for this category with the Kessler scheme and WRF Single-moment 3-class microphysics scheme combined with MM5 Similarity scheme for surface layer options. The radiation physics were taken as CAM shortwave and longwave schemes, RRTMG shortwave and longwave schemes and Fu–Liou–Gu shortwave and longwave schemes, and Kain–Fritsch scheme was selected for the cumulus parameterization option for all the three tests of this category. Table 3 shows three different combinations of the physics parameters with RUC Land Surface model.

RESULTS AND DISCUSSION

Temperature

The WRF-simulated 2 m air temperature data were averaged over the testing period (May, June, July, August of 2009) and compared with the ANUSPLIN temperature data for the same period. The ANUSPLIN data are daily observational

Table 1 | Physics options used with 5-layer Thermal Diffusion scheme (sf_surface_physics = 1)

Test No.	mp_physics	ra_lw_physics	ra_sw_physics	sf_sfclay_physics	bl_pbl_physics	cu_physics
1	3	1	1	1	1	1
2	4	4	4	1	1	1
3	2	4	4	1	7	1

Table 2 | Physics options used with Unified Noah Land Surface model (sf_surface_physics = 2)

Test No.	mp_physics	ra_lw_physics	ra_sw_physics	sf_sfclay_physics	bl_pbl_physics	cu_physics
4	2	5	5	1	1	1
5	3	5	5	1	1	1
6	3	4	4	1	1	1
7	3	1	1	1	1	1
8	3	3	3	1	1	1
9	2	3	3	1	1	1
10	2	4	4	2	2	1
11	6	3	3	1	1	1
12	16	3	3	1	1	1
13	1	7	7	10	10	6
14	4	4	4	2	2	2
15	2	1	1	1	1	2

Table 3 | Physics options used with RUC Land Surface model (sf_surface_physics = 3)

Test No.	mp_physics	ra_lw_physics	ra_sw_physics	sf_sfclay_physics	bl_pbl_physics	cu_physics
16	3	3	3	1	3	1
17	3	7	7	1	3	1
18	3	7	7	1	3	1

climate data produced by Natural Resources Canada and are available at 300 arc second (10 km) spatial resolution over Canada from 1950 to 2015. ANUSPLIN has been used as the source data to compare climate products (Eum *et al.* 2014; Wong *et al.* 2017) and to evaluate the accuracy of regional climate models (Eum *et al.* 2012) for Canada. Temperature bias over the basin was calculated and is shown in Figure 2. For the first category of WRF test (exp. no. 1 to 3), it was observed that using the 5-layer Thermal Diffusion scheme temperature was well simulated, although for test no.1 cold bias was observed up to −5 °C in the lake region; whereas exp. no. 2 and 3 show 1 to 3 degree positive bias in the lake region and slightly negative bias (up to −1 degree) in the north-western part of the basin. Figure 2 shows the 2 m air temperature bias (WRF-ANUSPLIN) over the MRB for MJJA 2009.

Using the Unified Noah Land Surface model in combination with other physics parameters (exp. no. 4–15) relatively higher temperature bias was obtained. In the experiments 4 to 10, the MRB experienced up to 5 degree warm bias at the north-eastern part of the basin excluding the lakes. The lake temperature showed around 1 °C negative bias. In the middle part of the basin, the positive bias tended to decrease gradually and become negative over the mountainous area of the basin. A similar pattern continued for different combinations of setup using the Noah model. In this category, exp. no. 11 and 12 showed promising results for simulating the summer temperature over the MRB.

For the third category (exp. 16, 17, and 18), only experiment 18 provided comparative results, while experiments 16 and 17 produced high temperature bias (WRF-ANUSPLIN).

It was observed that the temperature bias tended to increase from low to high from the western part of the basin to the eastern part, although the lake temperature was not captured perfectly for most of the cases. The basin has colder air temperature over the mountainous region which extended to further north, and this spatial distribution of temperature was successfully modeled by the WRF exp. no. 11. Results were promising in simulating the summer temperature and hence the setup for exp. no. 11 is considered as the fine-tuned WRF model setup.

The simulated 2 m air temperature using 18 different WRF setups was compared with the ERA-Interim temperature data, which were 0.5×0.5 degree resolution with the same time interval as that of WRF outputs. The 2 m air temperature from WRF and from ERA-Interim data were averaged over the basin area (52° N to 70° N and 140° W to 102° W) and then compared for summer 2009. Figure 3 shows the plotting of average 2 m air temperature from the ERA-Interim data and from the 18 different WRF experiments.

From Figure 3 it can be stated that exp. no. 11 and 12 showed close agreement with the reference ERA data.

A Taylor diagram (Taylor 2001) was plotted using the 18 different WRF simulations and the ERA-Interim dataset to show the statistical relationships between them. Figure 4 shows the correlation, RMSD, and standard deviation for each simulation (the numbers on the plot indicate the WRF experiment numbers). From Figure 4 it can be observed that exp. no. 11 and 12 have high correlations (0.8) and RMSD is about 3.2, whereas the standard deviation was above 5 for both of the cases.

From the analysis it was observed that the WRF model has significant dependence on the land surface model for simulating summer temperature. In our cases, Noah Land Surface model combined with the CAM shortwave and longwave schemes and MM5 Similarity Surface Layer scheme produced good temperature distributions, particularly with the WRF Single-moment or Double-moment 6-class microphysics scheme (exp. no. 11). The results were comparable

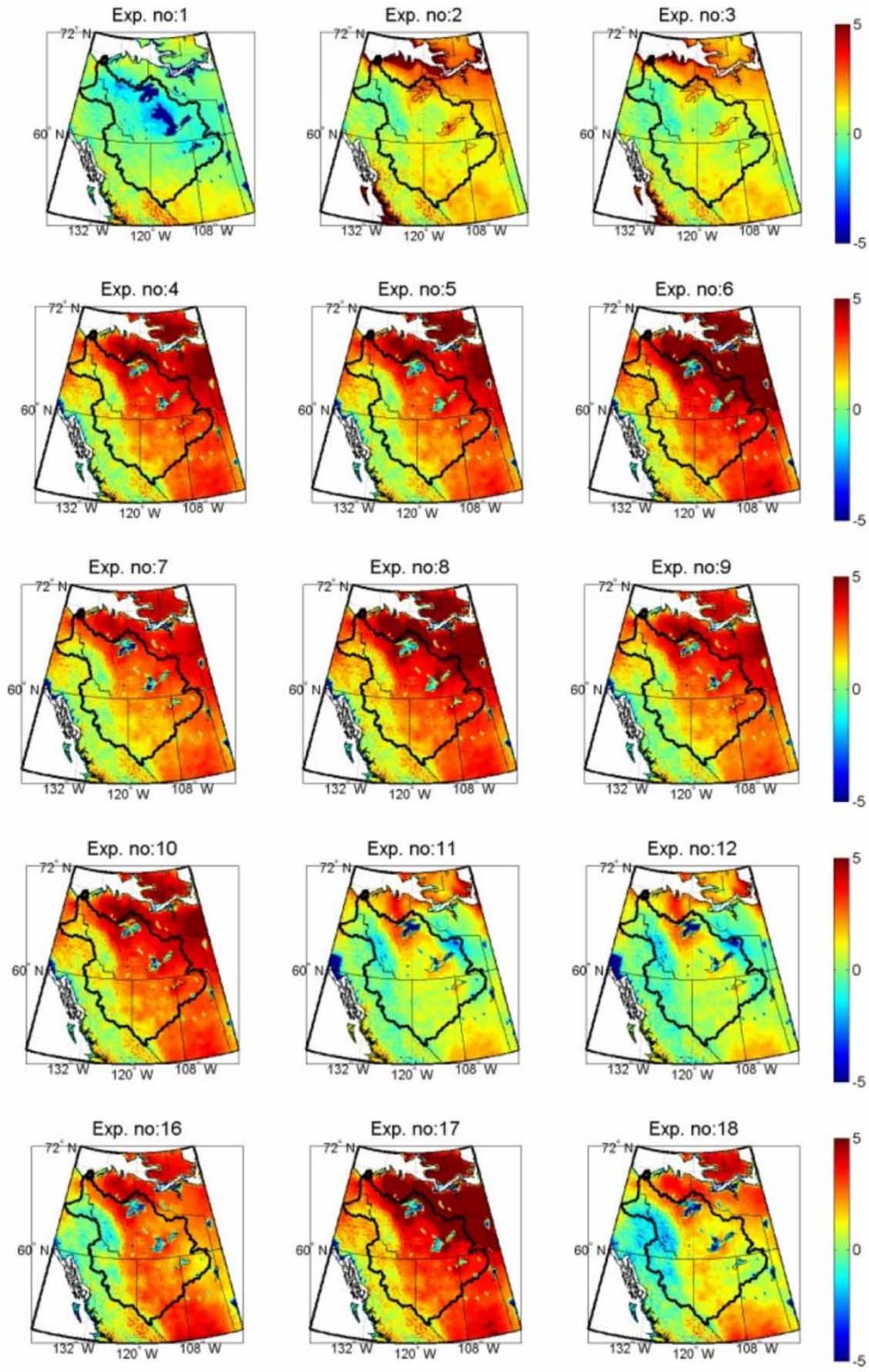

Figure 2 | Air temperature bias in degree Celsius (WRF-ANUSPLIN) for MJJA 2009.

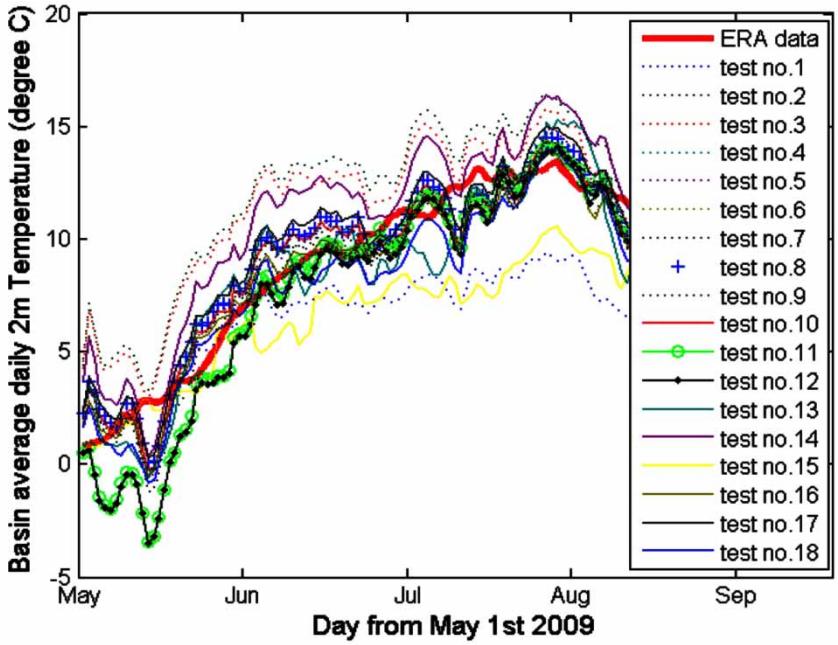

Figure 3 | Average 2 m temperature over the MRB for MJJA 2009.

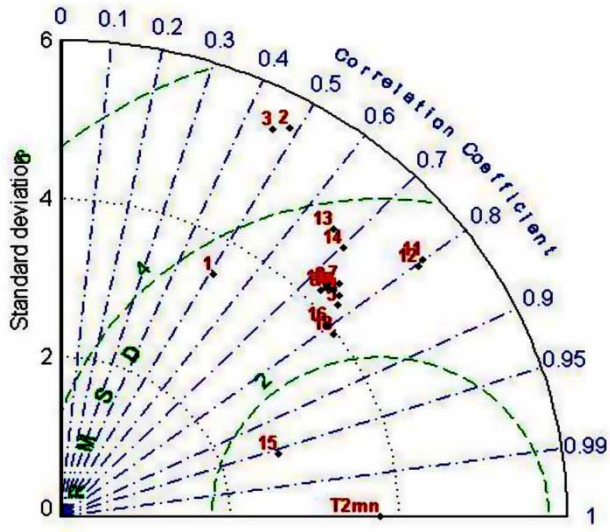

Figure 4 | Taylor diagram plot using the WRF experiments (exp. no. 1 to 18) and ERA-Interim data at 0.5 × 0.5 grid.

with the ANUSPIN data as well as with the ERA-Interim data. Mooney *et al.* (2013), who simulated the summer temperature over the Iberian Peninsula using different combinations of physics concluded that the combination of CAM longwave radiation and NOAH LSM produced better results for their cases. Similar findings were obtained by Jin *et al.* (2010).

Rainfall analysis

Summer (MJJA) 2009 rainfall was simulated using WRF and compared with the gridded ANUSPLIN rainfall data. To obtain uniform grid spacing, horizontal re-gridding was done and bias was plotted over the study domain to capture spatial variation of rainfall.

From exp. no 1, 2, and 3 it was observed that negative bias was dominant over the basin area, which goes up to 300 mm. However, a portion of the mountainous region experienced some positive bias for this group of experiments.

Results from WRF using the Unified Noah Land Surface model in combination with other physics parameters (exp. no. 4 to 15) provided better agreement with the gridded ANUSPLIN data although negative bias was dominant. Average negative bias for this category was found around 150 mm for summer 2009. It was observed that exp. no. 9–12 and 15 and 16 produced reasonable results where the WRF simulated rainfall was very close to the reference data. Microphysics option 3 (WRF Single-moment 3-class

scheme), 6 (WRF Single-moment 6-class scheme), and 16 (WRF Double-moment 6-class scheme) were used for experiment 8, 11, and 12, respectively. From the analysis it was recognized that microphysics in combination with the radiation physics, land surface physics, and cloud physics played an important role for simulating the MRB summer rainfall.

For the third category of WRF setup using the RUC Land Surface model it was observed that exp. no. 16 and 17 produced positive rainfall bias up to 300 mm over the mountainous region although the other parts of the basin experienced around 100 mm negative rainfall bias. For exp. no. 18, more negative rainfall bias was observed all over the basin. In exp. no. 16 and 17, WRF Single-moment 3-class microphysics scheme was used but for the radiation scheme CAM shortwave and longwave schemes were used in exp. no. 16, whereas Fu–Liou–Gu shortwave and longwave scheme was used for exp. 17. Figure 5 shows bias (WRF-ANUSPLIN) plotting for MJJA 2009 for exp. no 1 to 18, respectively.

Depending on the basis of the 18 experiments, it was found that the summer rainfall from exp. no. 11 and 12 agreed well with the ANUSPLIN 10 km gridded data. From the spatial distribution of rainfall pattern, it is clear that the model has a tendency to produce higher rainfall over the mountainous region while giving lower rainfall over the northern part of the basin.

To compare the WRF rainfall with the observed rain gauge data, eight climate stations located within the three major physiographic regions of the basin were selected. These eight stations were scattered over the MRB sub-basins, thus representing the different parts of the basin. The 'Second Generation of Daily Adjusted Precipitation for Canada' was collected from Environment Canada web site to use as the reference data. Figure 6 shows the selected rainfall station location over the MRB. Figure 7(i–ix) shows the plotting of cumulative rainfall for MMJA 2009 for different WRF experiments and the station rainfall at 1, 6, and 8. For the other stations, rainfall analysis and plotting are not shown here. It was observed that WRF simulations using exp. no. 11, 12, and 16 were able to produce comparable results at stations 1, 6, 7, and 8, but they produced higher rainfall at stations 2, 3, and 4 compared with the observed data. At station 5 all the WRF setups simulated lower rainfall value than the observed, although experiment 16 produced comparable rainfall here.

From the WRF outputs for summer 2009 rainfall it was observed that exp. no. 11, 12, and 16 provided comparable results with respect to ANUSPLIN rainfall data. These results were also comparable with the 'Second Generation of Daily Adjusted Precipitation' data for the selected stations. Experiment 11 was capable of capturing the main feature of summer rainfall and also was able to simulate the realistic distribution of rainfall pattern over the MRB. The physics options used for experiment no. 11 was WRF Single-moment 6-class scheme for the microphysics, Unified Noah Land Surface Model, CAM shortwave and longwave schemes, Yonsei University scheme (YSU) for planetary boundary layer physics, and Kain–Fritsch scheme for cumulus parameterization.

Albedo

For the MRB, WRF simulated albedo was compared with the ERA-Interim albedo data. The ERA-Interim albedo data were available in 0.5×0.5 degree grid with 6 hourly time steps. WRF albedo and the ERA-Interim albedo data were averaged over the MRB basin area and compared for MJJA 2009. Figure 8 shows that WRF simulated albedo mostly falls in the range from 0.15 to 0.25, whereas the ERA-Interim albedo is situated below the 0.15 line. Using the NIR (0.85 μm) spectral range for both MODIS and AVHRR data, the summer albedo was observed to vary from 0.15 to 0.25, and the months August–September give the minimum albedo for most of the cases (from 2000 to 2004). The above-stated measurement of albedo data supports our WRF simulated albedo results. Figure 8(a) shows the basin average albedo from 18 WRF simulations and from the ERA data for summer 2009. The Taylor diagram plotted in Figure 8(b) using the 18 WRF albedo and the ERA albedo data, showed that the exp. no. 11 and 12 were giving higher correlation coefficient although their RMSD and standard deviations were higher than others.

Surface pressure

WRF simulated mean surface pressure (PSFC) was compared with the ERA-Interim surface pressure over the

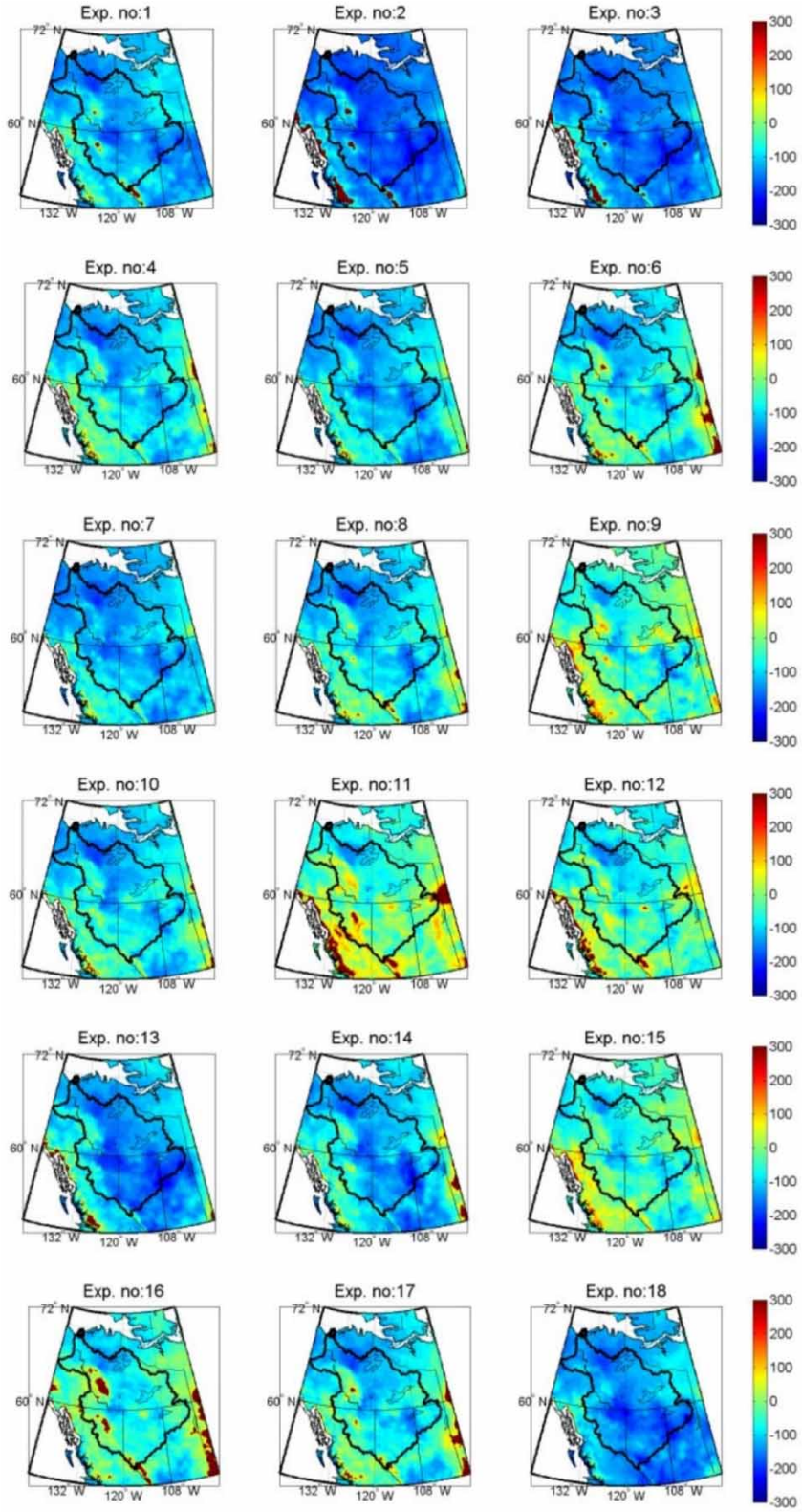

Figure 5 | Total precipitation bias in mm (WRF_ANUSPLIN) for MJJA 2009.

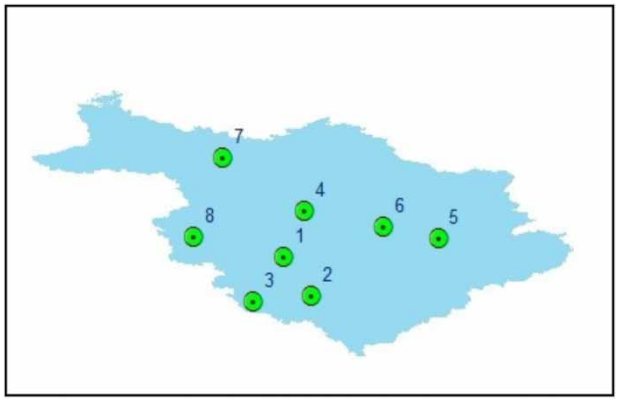

Figure 6 | Selected rainfall stations.

MRB for the MJJA 2009 period. Figure 9(a) shows the simulated mean surface pressure and the ERA mean surface pressure. It was observed that WRF consistently underestimates PSFC in summer for all the 18 experiments. Similar results were observed by Mooney *et al.* (2013), who found WRF produced consistent undersimulations for mean sea level pressure using different WRF setups. In our simulations, all the results were below the ERA data for simulating the surface pressure. The Taylor diagram also showed poor correlations and high RMSD for PSFC simulations. It was reported by Mooney *et al.* (2013) that the CAM radiation scheme performed better in comparison with the RRTM scheme; the same statement was true in our case as well.

Historical climate simulation

WRF experiment no. 11 was selected as the fine-tuned WRF setup for the study. This WRF setup was used to perform long-term simulations. ERA-Interim reanalysis data were used to downscale the climate of MRB at 6 hourly intervals and 30 km × 30 km resolution for multiple years from 1979 to 1991 for MJJASO period. The simulated temperature and rainfall data were compared with the high resolution (10 km × 10 km) daily ANUSPLIN data. The results of 2 m air temperature are shown in Figure 10. It was found that the WRF outputs for 2 m mean air temperature matched closely with the ANUSPLIN 2 m air temperature data, although negative bias was observed on the mountainous side of MRB.

We also compared the simulated rainfall for MJJASO of 1979–1991 with the ANUSPLIN data. From Figure 11 it can be observed that WRF rainfall has positive bias, especially over the mountainous area. Maussion *et al.* (2011) stated that WRF could capture the complex interactions between land and lower atmospherics in relatively horizontal terrains, but tends to suffer either over- or undersimulation problems in mountainous terrains; in our case, similar observations were made as WRF simulated rainfall was higher over the mountains.

Evaluation of the CanESM2 historical data downscaled by WRF

The CanESM2 model raw data 2.81° × 2.81° for MJJASO of the historical period from 1979 to 2005 were taken to dynamically downscale, using the selected WRF model setup. The input data for the WRF model were pre-processed at 6 hourly time intervals. The necessary initial and boundary conditions were set up using the WRF Preprocessing System (WPS); the land use data for MRB were taken from the USGS-based land use data set with inland water bodies (usgs_lakes) as the input to the geogrid field.

The selected WRF configuration (exp. no. 11) was used to downscale the CanESM2 air temperature and the rainfall data for MJJASO from 1979 to 2005 over the MRB. The outputs from the WRF model were at 30 km by 30 km in horizontal resolution with 6 hourly time steps. Figure 12 shows the comparison of WRF simulated 2 m temperature using the CanESM2 data for MJJASO during 1979 to 2005 with the re-gridded ANUSPLIN data for the same period.

The results showed that the spatial distribution of 2 m air temperature captured by WRF were reasonably good although the Rockies have undersimulation problems. For the eastern and central part of MRB with relatively flat terrain, the simulated air temperature showed close agreement with the ANUSPLIN data, even though there was some positive or negative bias. As expected, simulating climate processes in a complex, mountainous terrain is more challenging than simulating climate processes in a flat terrain. Dasari *et al.* (2014) found significant bias and poor correlation in air temperature simulated by WRF over complex topographic areas of Europe. A major source of this bias could be due to a lack of representative

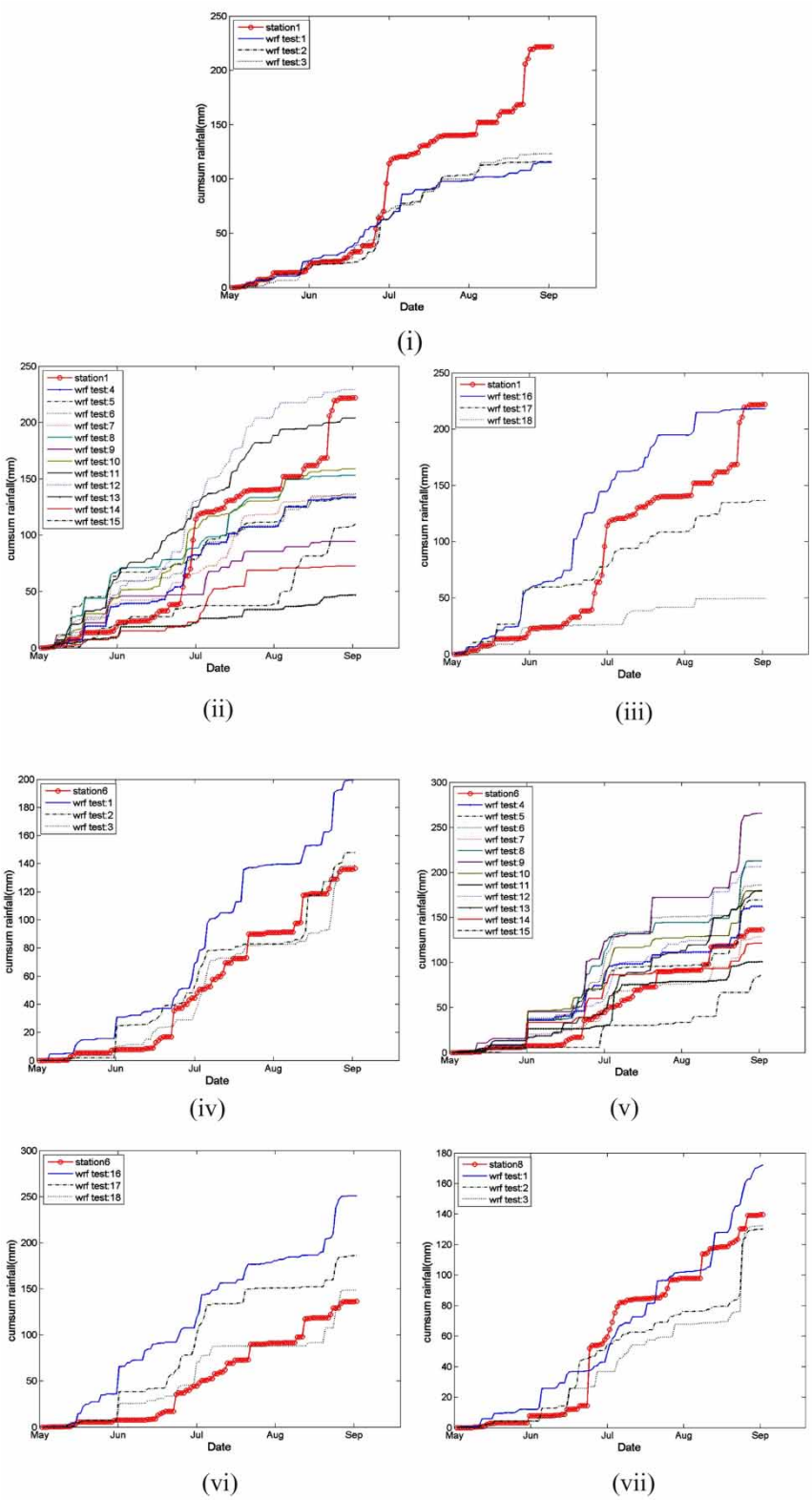

Figure 7 | Total rainfall plotting in mm at the station locations over MRB for MJJA 2009. (*continued*).

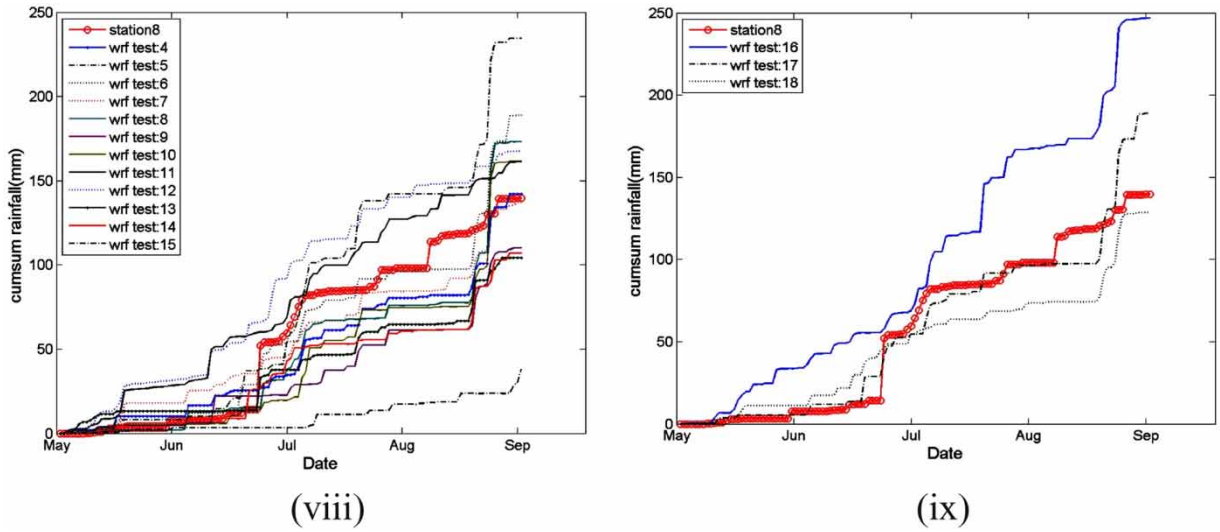

Figure 7 | continued.

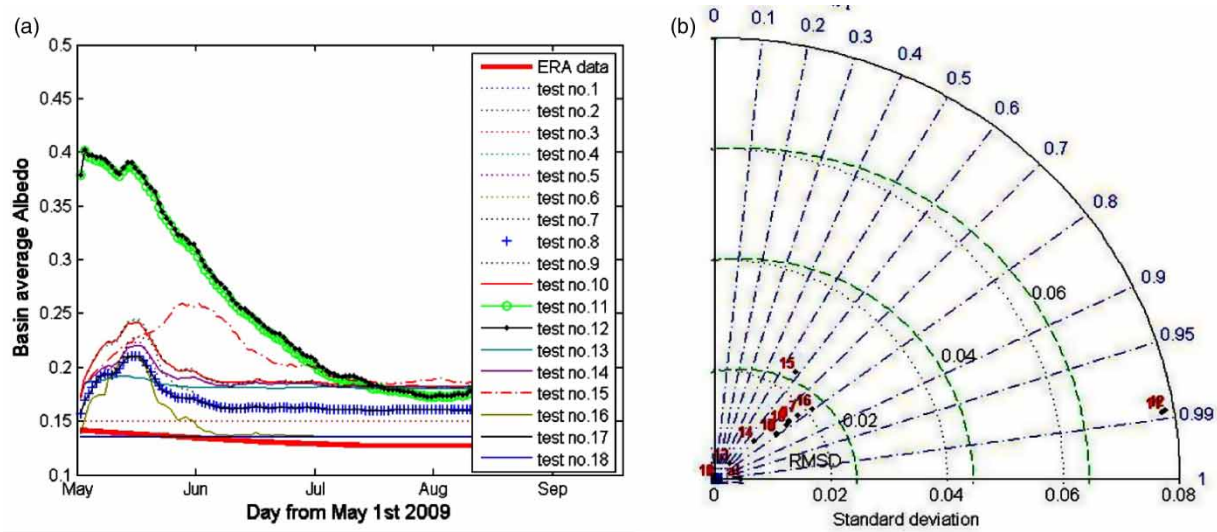

Figure 8 | (a) Average albedo over the MRB for MJJA 2009; (b) Taylor diagram plot using the WRF experiments (exp. no. 1 to 18) and ERA-Interim data at 0.5 × 0.5 grid.

topography and complex land surface–atmosphere interactions.

We also compared the ERA-Interim 2 m air temperature with WRF simulation over the same period. Figure 13 shows the bias plot for WRF and ERA-Interim data. A scatter plot of these temperature data is shown in Figure 14. The correlation coefficient was 0.81, which indicates a fairly good correlation between WRF simulations versus the ERA-Interim 2 m air temperature data.

To assess WRF simulated precipitation over the MRB for the historical period using CanESM2 data we compared the outputs with some observed station rainfall data. It was found that WRF simulated historical average rainfall data matches reasonably well with some observed rainfall data for summer (MJJASO) 1979–2005. At the Barkerville station (53°04′ N 121°30′ W), the average MJJASO precipitation has been about 556 mm from the precipitation chart of Canadian Climate Normals (CCN) for 1971 to 2000, while

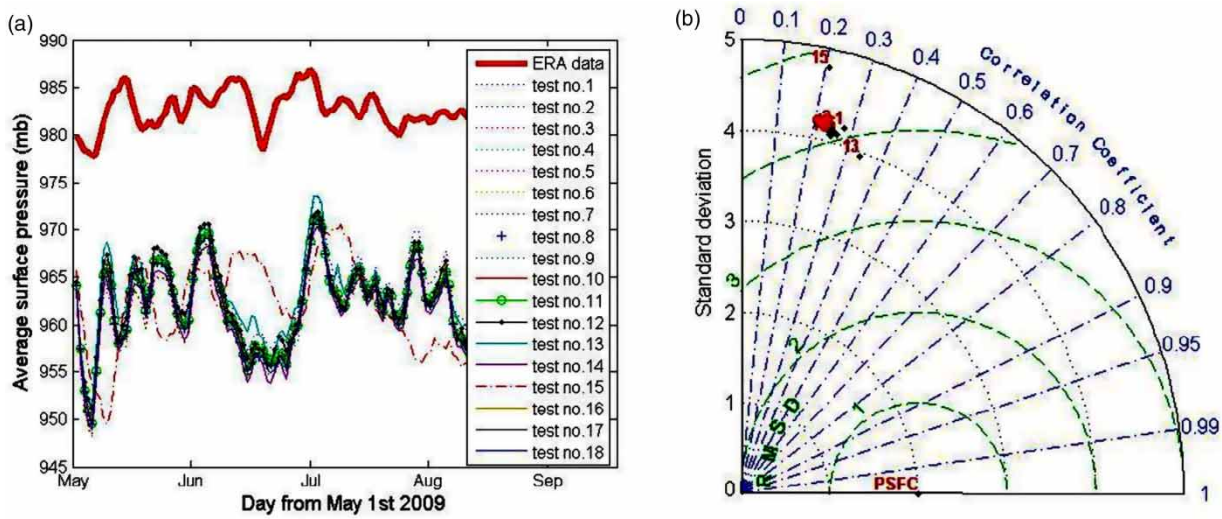

Figure 9 | (a) Mean surface pressure (PSFC) over the MRB for MJJA 2009; (b) Taylor diagram plot using the WRF experiments (exp. no. 1 to 18) and ERA-Interim data at 0.5 × 0.5 grid.

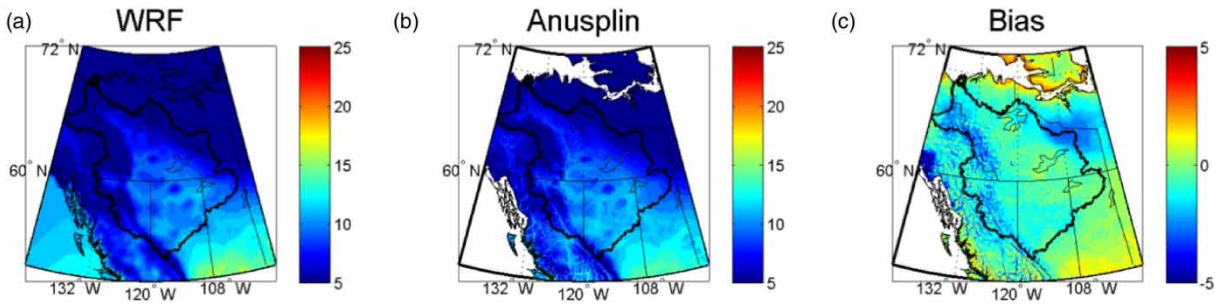

Figure 10 | (a) Average 2 m air temperature from WRF output for MJJASO of 1979 to 1991; (b) 2 m air temperature from ANUSPLIN data for the same period; (c) 2 m air temperature bias (WRF-ANUSPLIN).

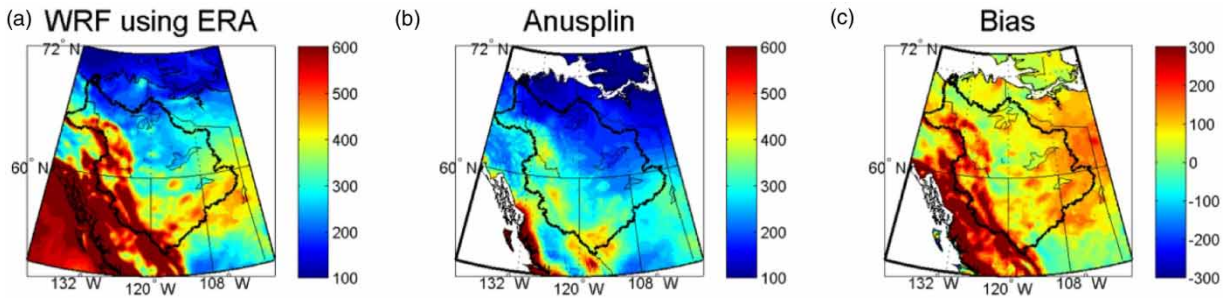

Figure 11 | (a) Average rainfall from WRF simulations for MJJASO 1979 to 1991; (b) average rainfall from ANUSPLIN data for the same period; (c) average rainfall bias.

WRF simulated average rainfall was about 540 mm for MJJASO over 1979–2005. Similarly for the Hay River station 60°50′) N 115°46′ W), it was 237.2 mm (CCN) versus 255 mm WRF rainfall for the same period; and for the Norman Wells A (65°16′ N 126°48′ W) it was 205.1 mm (CCN) versus 200 mm (WRF) and for Yellowknife A (62°27′ N 114°26′ W) it was 194 mm (CCN) versus 200 mm (WRF).

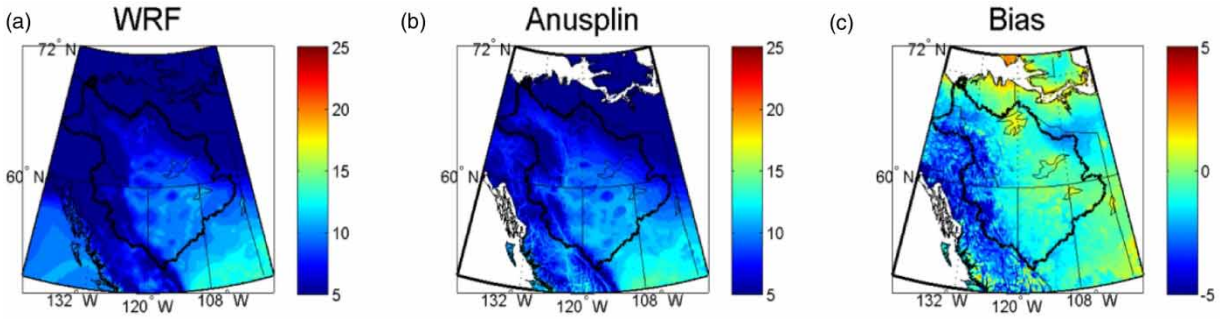

Figure 12 | (a) Average 2 m air temperature from WRF output using CanESM2 data for MJJASO of 1979 to 2005; (b) 2 m air temperature from Anusplin data for the same period; (c) bias.

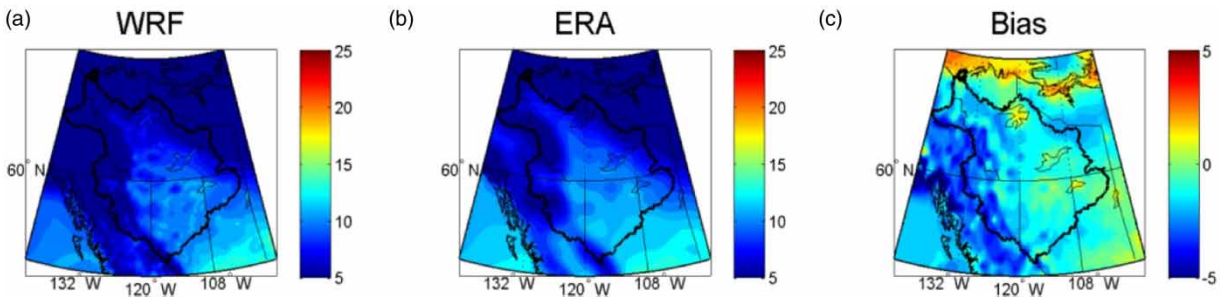

Figure 13 | (a) Average 2 m air temperature from WRF output using CanESM2 data for MJJASO of 1979 to 2005; (b) 2 m air temperature from ERA-Interim data for the same period; (c) bias.

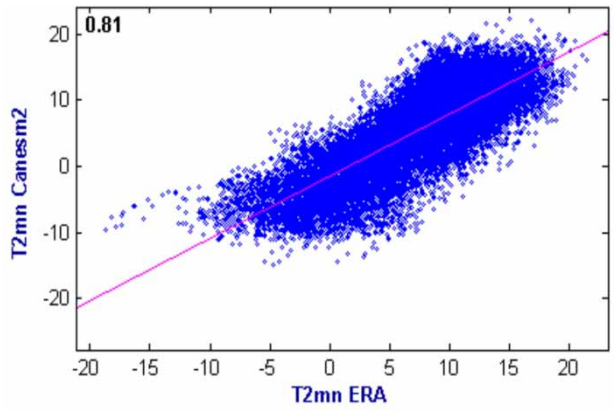

Figure 14 | Scatter plot of WRF simulated temperature from the CanESM2 historical 1979–2005 temperature data and the ERA-Interim 2 m temperature.

From Figure 15, it was observed that most of the mountainous area has much higher precipitation than the low lying plains of central and eastern parts of MRB. It was also noticeable that WRF oversimulated precipitation over the western part of the MRB, but it produced reasonable precipitation over other parts of the MRB for the historical period. By comparing with the ANUSPLIN data, it was clear that the bias of WRF simulation was generally modest although about 250 mm of positive bias in the western part and about 100 mm in the north-eastern part of the MRB were observed.

Based on 2 m air temperature and precipitation data from WRF simulations for the base period (1979–2005) using CanESM2 historical data or from the ERA-Interim reanalysis data (for 1979–1991), it was found that the chosen WRF setup (exp. no. 11) was suitable for long-term summer temperature and rainfall simulations for MRB.

CONCLUSIONS

In this study, a physically based mesoscale model called WRF was tested for 18 different physics combinations to simulate the climate of MRB. The outputs from the WRF were compared and analyzed with the reference data to investigate the sensitivity of the model parameters and significant sensitivity was found; especially to microphysics, land surface, planetary boundary layer, and longwave radiation schemes. Temperature, rainfall, albedo and surface

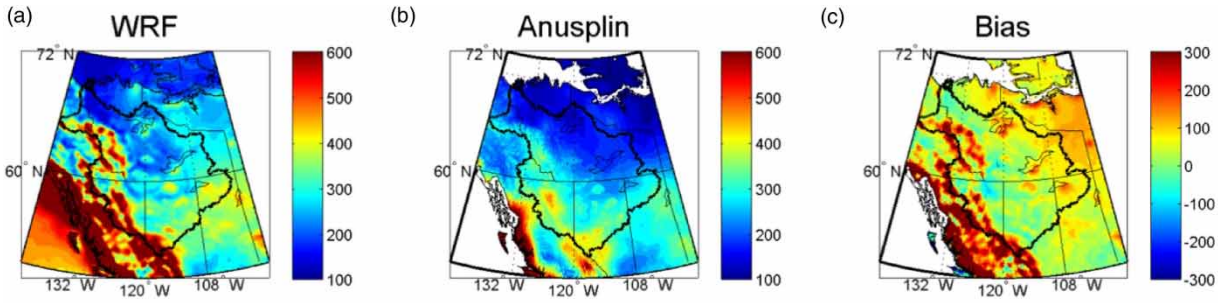

Figure 15 | (a) Average rainfall from WRF output using CanESM2 for MJJASO of 1979 to 2005; (b) average rainfall from ANUSPLIN data for the same period; (c) bias.

pressure were simulated by WRF for summer 2009 as a testing period and compared with the reference value. From the 18 different WRF experiments, we found that exp. no. 11 produced comparable results. Noah Land Surface Model, WRF Single-moment 6-class scheme for the microphysics, CAM shortwave and longwave schemes, Yonsei University Scheme (YSU) for planetary boundary layer physics, Kain–Fritsch scheme for cumulus parameterization were used as the physics parameters for exp. no. 11.

It was observed that the WRF simulated precipitation from experiment 11 had good agreement with the reference data although some positive bias (WRF-ANUSPLIN) was observed over the mountainous region and negative bias for the other parts of the basin. We found that the special variability of rainfall distribution over the basin was more realistically captured by exp. no. 11.

In the case of air temperature simulation, WRF showed high proficiency in simulating the summer 2009 temperature using the Noah Land Surface Model. It was observed that exp. no. 11 could realistically downscale the surface air temperature. Also, the spatial variability of temperature distribution over the MRB was well captured by WRF. We found that the temperature simulation was sensitive to land surface model, microphysics, and radiation schemes.

We also compared the WRF simulated albedo with the observed albedo data as well as with the ERA albedo data, and good results were found.

However, the mean surface pressure (PSFC) simulated by WRF showed continuous undersimulation in comparison to ERA-Interim data, which was a similar finding from others.

This study provided a guideline for the selection of model parameters to simulate the climate for a large and complex area. The proposed WRF setup from this study was utilized to simulate long-term climate over MRB for the base period. WRF simulations for the summer period from 1979 to 1991 based on ERA-Interim reanalysis data were compared with the ANSUPLIN data and the ERA data, which showed good agreement. The current WRF setup was further utilized to downscale MRB climate (air temperature and rainfall) using CanESM2 data for the base period (summer 1979–2005), and reliable results were obtained by comparing with the reference data for the same period. From this study, the recommended WRF parameterizations would be useful for regional climate modeling and for future climate change projection of that area.

ACKNOWLEDGEMENTS

We thank Dr Chun-Chao Kuo for his support, Transport Canada for funding this study, Environment Canada, NCEP, and ECMWF for the use of their data source, WestGrid supercomputing program and the wrf-model.org.

DATA AVAILABILITY STATEMENT

Data cannot be made publicly available; readers should contact the corresponding author for details.

REFERENCES

Chawla, I., Osuri, K. K., Mujumdar, P. P. & Niyogi, D. 2018 Assessment of the weather research and forecasting (WRF) model for simulation of extreme rainfall events in the upper Ganga Basin. *Hydrology Earth System Science* **22**, 1095–1117.

Dasari, H. P., Salgado, R., Perdigao, J. & Challa, V. S. 2014 A regional climate simulation study using WRF-ARW model over Europe and evaluation for extreme temperature weather events. *International Journal of Atmospheric Sciences* **13**, 1–22.

Eum, H. I., Gachon, P., Laprise, R. & Ouarda, T. 2012 Evaluation of regional climate model simulations versus gridded observed and regional reanalysis products using a combined weighting scheme. *Climate Dynamics* **38** (7–8), 1433–1457.

Eum, H. I., Dibike, Y., Prowse, T. & Bonsal, B. 2014 Inter-comparison of high-resolution gridded climate data sets and their implication on hydrological model simulation over the Athabasca Watershed, Canada. *Hydrological Processes* **28** (14), 4250–4271.

Gula, J. & Peltier, W. R. 2012 Dynamical downscaling over the Great Lakes basin of North America using the WRF regional climate model: the impact of the Great Lakes system on regional greenhouse warming. *Journal of Climate* **25** (21), 7723–7742.

Jin, J., Miller, N. L. & Schlegel, N. 2010 Sensitivity study of four land surface schemes in the WRF model. *Advances in Meteorology* **2010**, 1–11.

Maussion, F., Scherer, D., Finkelnburg, R., Richters, J., Yang, W. & Yao, T. 2011 WRF simulation of a precipitation event over the Tibetan Plateau, China– an assessment using remote sensing and ground observations. *Hydrology Earth System Science* **15**, 1795–1817.

Mooney, P. A., Mulligan, F. J. & Fealy, R. 2013 Evaluation of the sensitivity of the weather research and forecasting model to parameterization schemes for regional climates of Europe over the period 1990–95. *Journal of Climate* **26** (3), 1002–1017.

Pei, L., Moore, N., Zhong, S., Luo, L., Hyndman, D. W., Heilman, W. E. & Gao, Z. 2014 WRF model sensitivity to land surface model and cumulus parameterization under short-term climate extremes over the southern great plains of the United States. *Journal of Climate* **27** (20), 7703–7724.

Pérez, J. C., Díaz, J. P., González, A., Expósito, J., Rivera-López, F. & Taima, D. 2014 Evaluation of WRF parameterizations for dynamical downscaling in the Canary Islands. *Journal of Climate* **27** (14), 5611–5631.

Prabha, T. V., Hoogenboom, G. & Smirnova, T. G. 2011 Role of land surface parameterizations on modeling cold-pooling events and low-level jets. *Atmospheric Research* **99** (1), 147–161.

Taylor, K. E. 2001 Summarizing multiple aspects of model performance in a single diagram. *Journal of Geophysical Research: Atmospheres* **106** (D7), 7183–7192.

Wong, J. S., Razavi, S., Bonsal, B. R., Wheater, H. S. & Asong, Z. E. 2017 Inter-comparison of daily precipitation products for large-scale hydro-climatic applications over Canada. *Hydrology and Earth System Sciences* **21** (4), 2163–2185.

Woo, M. K., Rouse, W. R., Stewart, R. E. & Stone, J. M. 2008 The Mackenzie GEWEX Study: a contribution to cold region atmospheric and hydrologic sciences. In: *Cold Region Atmospheric and Hydrologic Studies: The Mackenzie GEWEX Experience* (M. K. Woo, ed.). Springer, Berlin, Heidelberg, Germany.

Yang, Q., Dai, Q., Han, D., Chen, Y. & Zhang, S. 2019 Sensitivity analysis of raindrop size distribution parameterizations in WRF rainfall simulation. *Atmospheric Research* **228**, 1–13.

Zhang, C., Wang, Y., Lauer, A. & Hamilton, K. 2012 Configuration and evaluation of the WRF model for the study of Hawaiian regional climate. *Monthly Weather Review* **140** (10), 3259–3277.

First received 14 February 2020; accepted in revised form 13 May 2020. Available online 9 July 2020